Dipole-Dipole Excitation and Ionization in an Ultracold Gas of Rydberg Atoms

Wenhui Li, Paul J. Tanner, and T. F. Gallagher
Department of Physics, University of Virginia, Charlottesville, Virginia 22904, USA
(Received 30 November 2004; published 4 May 2005)

In cold dense Rydberg atom samples, the dipole-dipole interaction strength is effectively resonant at the typical interatomic spacing in the sample, and the interaction has a $1/R^3$ dependence on interatomic spacing R. The dipole-dipole attraction leads to ionizing collisions of initially stationary atoms, which produces hot atoms and ions and initiates the evolution of initially cold samples of neutral Rydberg atoms into plasmas. More generally, the strong dipole-dipole forces lead to motion, which must be considered in proposed applications.

DOI: 10.1103/PhysRevLett.94.173001 PACS numbers: 32.80.Pj, 34.60.+z

Cold Rydberg gases are of interest for two reasons. First, on the 1 μs time scale of experimental interest, the 300 μK atoms move 0.3 μm, roughly 3% of the average interatomic spacing at a density of 10^9 cm^{-3}, so the gas appears to be frozen and is, in effect, a disordered solid [1–6]. At this density, normal atoms are noninteracting. However, due to their large dipole moments, scaling as n^2, where n is the principal quantum number, the Rydberg atoms interact, and they constitute an artificial solid with controllable properties. For this reason, dipole-dipole interactions between cold Rydberg atoms have been suggested as the basis for gates for quantum computing [7,8]. Second, cold Rydberg atom samples spontaneously evolve into ultracold plasmas, and ultracold plasmas recombine to form Rydberg atoms [9–12].

Until now these two topics have been viewed as distinct, but here we show that they are intimately connected. In particular, we show that resonant dipole-dipole interactions lead to a significant motion of some of the atoms, and this motion is responsible for initiating the spontaneous evolution into a plasma of cold samples of Rydberg atoms. Plasmas form spontaneously from cold Rydberg atom samples as follows [9]. The electrons resulting from an initial ionization process leave the trap volume but the cold ions remain. Once enough ions accumulate (typically $\sim$1000), their macroscopic positive charge traps subsequently produce electrons, which then quickly redistribute the Rydberg atom population by collisions. Roughly 2/3 of the initial Rydberg population is ionized to form the ultracold plasma; the remaining 1/3 is transferred to lower lying states, providing energy balance [13]. For low n states, the initial ionization comes from photoionization by 300 K blackbody radiation or collisions with residual 300 K Rydberg atoms. At high n, $n > 50$, even when there are no hot atoms, the evolution to a plasma occurs more quickly than at low n. This observation is incompatible with initial ionization by 300 K blackbody photoionization, and recent experiments showed that the rate for this process scales as n^4, although the mechanism was not clear [13]. Here we present evidence that the mechanism is the resonant dipole-dipole interaction which leads to ionization and the production of hot atoms and ions. We outline the essential ideas using a two-atom picture, describe our experiments, and discuss the implications.

The fundamental interactions between two neutral atoms are their electric multipole interactions, and the longest range of these is the dipole-dipole interaction [14]. Assuming there are no fields present, isolated atoms are in states of definite parity which have no permanent dipole moments, only transition dipole moments. If two atoms are in states which are of opposite parity and dipole connected, s and p states, for example, from the two atoms we can form two molecular states, sp and ps, which are degenerate at infinite separation but are shifted by $\pm\mu^2/R^3$ at any finite internuclear spacing R due to the resonant dipole-dipole interaction. Here μ is the $s-p$ transition dipole moment. Unless units are given explicitly, all quantities are expressed in atomic units. Although it is an oversimplification, we ignore orientational effects here and throughout this Letter. Because of the forces associated with these dipole-dipole potentials, especially the attractive one, motion of the atoms results, and it must be taken into account for cold atoms [15]. If, however, the two atoms are not in dipole coupled states, there is no first order interaction to lift the degeneracy as $R \rightarrow \infty$, and as $R \rightarrow \infty$ the interaction is usually a van der Waals interaction scaling as $1/R^6$, not as $1/R^3$.

Now consider a pair of Rb $46d$ Rydberg atoms separated by R. This pair of atoms in the $46d46d$ molecular state is dipole coupled to all molecular states in which the same atoms are in nf or np states. The most important couplings are the strong ones to the energetically nearby $48p44f$ and $47p45f$ states. For very large R, the dominant coupling is to the Rb $48p_{3/2}44f$ pair, which is removed in energy by $\Delta = 187$ MHz at $R = \infty$ [16] and has the two transition dipole moments $\mu_{dp} = 1548$ and $\mu_{df} = 1587$, which we calculate by the Numerov method [17]. From perturbation theory it is apparent that at very large R the $48p_{3/2}44f$ and $46d46d$ states will be shifted up and down in energy by $\pm(\mu_{df}\mu_{dp}/R^3)^2/\Delta$. Summing over all such terms gives the van der Waals interaction. From this dominant term, using $\mu_{df}\mu_{dp} \approx n^4$ and $\Delta \approx \delta/n^3$, we recover the n^{11} scal-

ing of the van der Waals interaction [14]. However, the van der Waals interaction is only valid for $\mu_{df}\mu_{dp}/R^3 \approx n^4/R^3 < \delta/n^3$, which translates into $R > R_{\rm vdw} = (n^7/\delta)^{1/3}$. For our case and several cases of interest, $\delta \leq 0.01$. For $\delta = 0.01$ and $n = 50$, $R_{\rm vdw} = 4.0 \times 10^4$, or $2.1\,\mu$m, which is comparable to the interatomic spacing in a trap.

There are many possible $48p44f$ and $47p45f$ pairs, but to represent essential physics, we simply consider the $47p_{3/2}45f$ pair in addition to the $48p_{3/2}44f$ pair. The $47p_{3/2}45f$ pair is removed from the $46d46d$ pair by $\Delta = 2.027$ GHz at $R = \infty$ and coupled to it by the two dipole moments $\mu_{dp} = 2709$ and $\mu_{df} = 2694$. In Fig. 1(a), we show the potential curves of $46d46d$, $48p_{3/2}44f$, and $47p_{3/2}45f$ pairs. A pair of atoms initially on the attractive curve are drawn to each other, collide, and ionize, providing the initial ionization required for the evolution to a plasma. If there are 10^5 atoms in a sphere of 0.1 mm radius, roughly 1500 atoms must be ionized to provide the macroscopic space charge needed for avalanche ionization. The most closely spaced 1500 atoms are spaced by $R < 1.7\,\mu$m and collide with each other in 300 ns, if the atoms move on the attractive dipole-dipole potential. An ion, an electron, and a more tightly bound atom are formed, and both the ion and the atom have speeds of $\sim 10^4$ cm/s, almost 3 orders of magnitude higher than the speed of cold Rydberg atoms.

The Rb ns state nearest to the $46d$ state is the $48s$ state. The nearest dipole coupled pair to the $48s48s$ pair is the $47p_{3/2}48p_{3/2}$ pair, which is removed by $\Delta = -2.756$ GHz at $R = \infty$. As shown by Fig. 1(b), $R_{\rm vdw} = 1.1\,\mu$m, and only for $R < 1.1\,\mu$m do these potentials become $1/R^3$ dipole-dipole potentials. Thus two $48s$ atoms are not as likely as $46d$ atoms to collide and ionize or to form a plasma. Two $48s$ atoms initially at $R = 1.7\,\mu$m require 500 ns to collide, which is a time long enough that a substantial fraction of the hot ions formed begins to leave the trap volume. The potential curves for the Rb $np_{3/2}$ states, which easily form plasmas, resemble the Rb $46d46d$ curves and not the $48s48s$ curves.

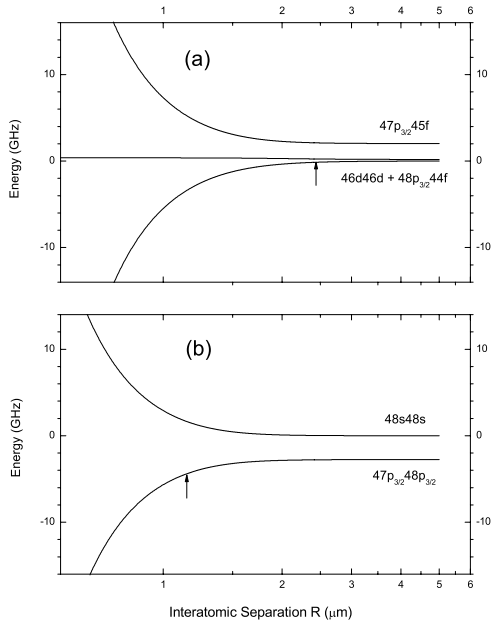

FIG. 1. (a) Potential energy curves for the coupled $46d46d$, $48p44f$, and $47p45f$ pairs. The dipole-dipole coupling exceeds the zero field $46d46d$-$48p44f$ splitting at $R_{\rm vdw} = 2.5\,\mu$m, shown by the arrow. Pairs on the attractive potential spaced by R less than $1.7\,\mu$m move to small separation, collide, and ionize in less than 300 ns. (b) Potentials for the $48s48s$ and $47p48p$ pairs. In this case, $R_{\rm vdw} = 1.1\,\mu$m, as shown by the arrow. Pairs on the attractive potential spaced by $1.7\,\mu$m require 500 ns to collide.

In our experiments we start with ^{85}Rb atoms in a vapor loaded magneto-optical trap, in which the atoms are at 300 μK and at a $5p_{3/2}$ density of 5×10^{10} cm^{-3} [18]. The atoms are excited from the $5p_{3/2}$ state to ns or nd Rydberg states at a 20 Hz repetition rate using a pulse amplified, frequency doubled 960 nm continuous wave Ti:sapphire laser. The laser pulses have a 10 ns duration, 20 μJ energy, and 200 MHz bandwidth, and the beam is focused to a 0.2 mm diameter waist in the trap volume. About 10% of the cold atoms are excited to Rydberg states, leading to a maximum density of Rydberg atoms of 5×10^9 cm^{-3}.

We have observed the plasma formation and population transfer to higher dipole coupled states starting from initially excited Rb ns and nd states as a function of Rydberg atom density and time delay after laser excitation. We analyze the final states of the atoms by applying a field ramp with a rise time of 2 μs. We can detect either ions or electrons. The ions or electrons in an ultracold plasma are detected at the beginning of the field ramp, and the atoms in a Rydberg state are detected after the ramped field reaches its ionization threshold [19]. In the time resolved signals, it is straightforward to observe ionization and state changing using electron detection. In Fig. 2, we show signals using electron detection taken with a 250 ns delay after laser excitation when we excite the Rb $46d$ and $48s$ states. The field ionization pulse amplitude is 99 V/cm. As shown in Fig. 2(a), for the $48s$ state at low density, there is one peak at 2.4 μs or 90 V/cm, the ionization field of the $48s$ state. At intermediate density there is transfer to the $48p$ state, resulting in the peak at 2.2 μs, and at high density there is more transfer to the $48p$ state but negligible transfer to high lying states and no plasma formation. As shown in Fig. 2(b), the $46d$ state at low density exhibits a qualitatively similar narrow peak at 2.4 μs, but the similarity ends there. At intermediate density there is substantial population transfer to the $48p$ state, which ionizes at 2.2 μs. At high density, the signal is very different. At $0.5\,\mu{\rm s} < t < 1.5\,\mu$s, there is a peak due to the plasma electrons; from 1.5 to 2 μs, the signal represents high n states, and the $48p$ state now appears as an early shoulder on the $46d$ signal at 2.2 μs. When a plasma has formed, its ions and electrons are swept past the Rydberg atoms by the field ionization pulse. While this can, in principle, blur the field ionization signal, there is no evidence that it does so to

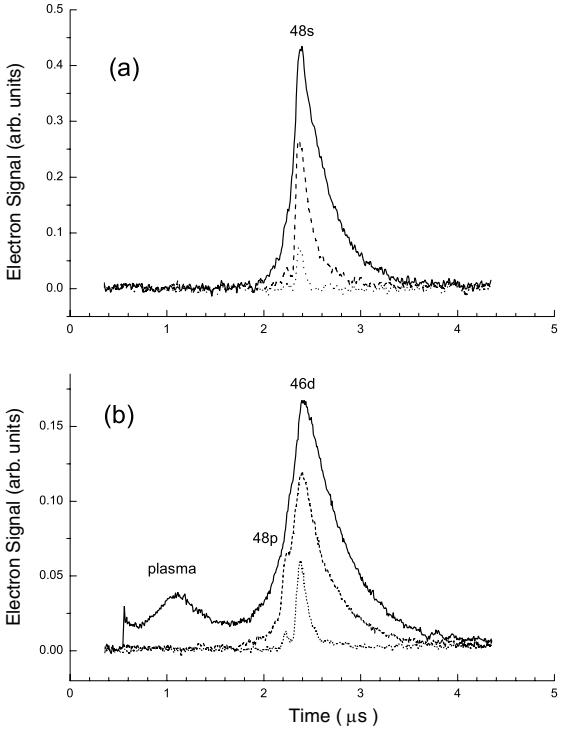

FIG. 2. Time resolved electron signals with the field ionization pulse 250 ns delayed from the laser excitations. (a) 48s initial state at density of 5×10^9 (solid line), 1.5×10^9 (dashed line), and 2×10^8 (dotted line) atoms/cm^3, respectively; (b) 46d initial state at density of 5×10^9 (solid line), 1.5×10^9 (dashed line), and 4×10^8 (dotted line) atoms/cm^3. The population transferred to the high angular momentum states while the plasma is formed is not seen in this spectrum due to the low field ionization field.

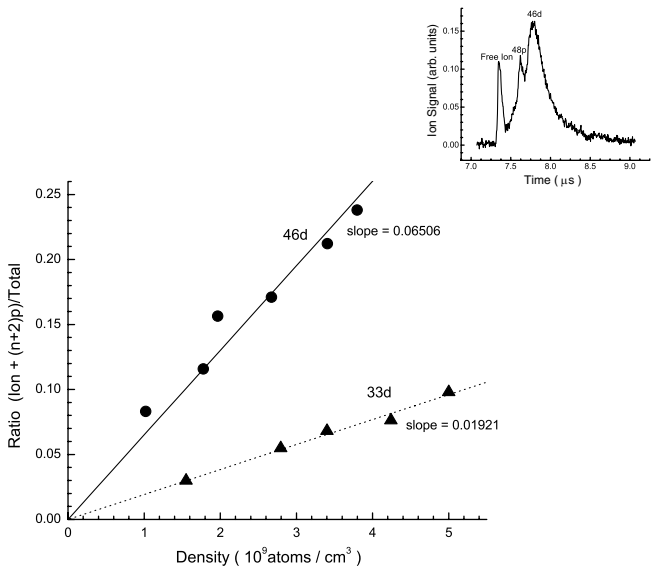

FIG. 3. Ratio of the free ion + $(n+2)p$ signals produced by the resonant dipole-dipole interaction to the total signal 250 ns after laser excitation of the 46d (●) and 33d (▲) states. The inset shows the time resolved signal for the 46d state when the total number of atoms is 5×10^9atoms/cm^3. The slopes of the ratios are linear in the number of atoms, as expected for a binary process, and the ratio of the slopes is 3.4, in agreement with the expected n^4 scaling.

a significant degree. As shown by Fig. 2, under the same conditions 46d and 48s atoms exhibit very different behavior, an observation completely consistent with the potential curves of Fig. 1.

The population transfer shown in Fig. 2 for the 46d state implicitly exhibits a nonlinear density dependence. Rather than plot the population transfer, which exhibits a quadratic variation with density, in Fig. 3 we plot the ratio of the combined $(n+2)p$ and free ion signals to the total signal for the Rb 46d and 33d vs density. The ratios exhibit the linear dependence on the total number of atoms excited expected for a binary process. Furthermore, the slope for the 46d state is 3.4 times as large as the slope for the 33d state, which is consistent with an n^4 scaling of the rate [13].

We interpret the plasma formation from initially excited 46d atoms to the motion along the attractive dipole-dipole potential shown in Fig. 1. We observe more ionization on the red side of the optical excitation of the 46d state than on the blue side, but our optical resolution is not adequate to show this phenomenon in a convincing way. However, ionization on the attractive dipole-dipole potential can be shown with unprecedented clarity using microwaves. To show this most clearly, we use as a starting point atoms in the 39s state, for they do not evolve into a plasma in less than 10 μs. In Fig. 4, we show the results of exposing Rb 39s atoms to a microwave pulse to drive the 39s-39$p_{3/2}$ transition. As shown in Fig. 4(a), we are really driving the molecular transition from the 39s39s state. The microwave pulse is 500 ns long and produces an on-resonance Rabi frequency of 50 MHz. Using a field pulse 1 μs after the laser pulse, we detect the free ions produced by colliding atoms as we sweep the microwave frequency over many shots of the laser. As shown in Fig. 4(b), we see a signal only on the low frequency side of the 39s-39$p_{3/2}$ transition at 68.378 GHz [16]; i.e., we see only transitions to the attractive dipole-dipole potential. If we drive the microwave transition down in energy to the 38$p_{3/2}$ state, we see an ion signal only on the high frequency side of the atomic transition frequency; the observed transition is again only to the attractive dipole-dipole potential curve. Finally, using the microwaves to make $ns - np$ mixtures, we can explicitly turn on the dipole-dipole interactions to see the effect on plasma formation. In Fig. 4(c), we show the time resolved electron signals, analogous to those of Fig. 2, detected 3.5 μs after the 39s state is populated with and without a microwave pulse to drive the 39s-39$p_{3/2}$ transition. In both cases shown in Fig. 4(c), the same number of 39s atoms is excited. Without the pulse, the population remains in the 39s state, but, with it, a plasma forms as shown by the signal at 0.5 μs, and there is obvious population transfer to other Rydberg states as well.

The fact that the strength of resonant dipole-dipole interactions rises as n^4, while the atomic energy level spac-

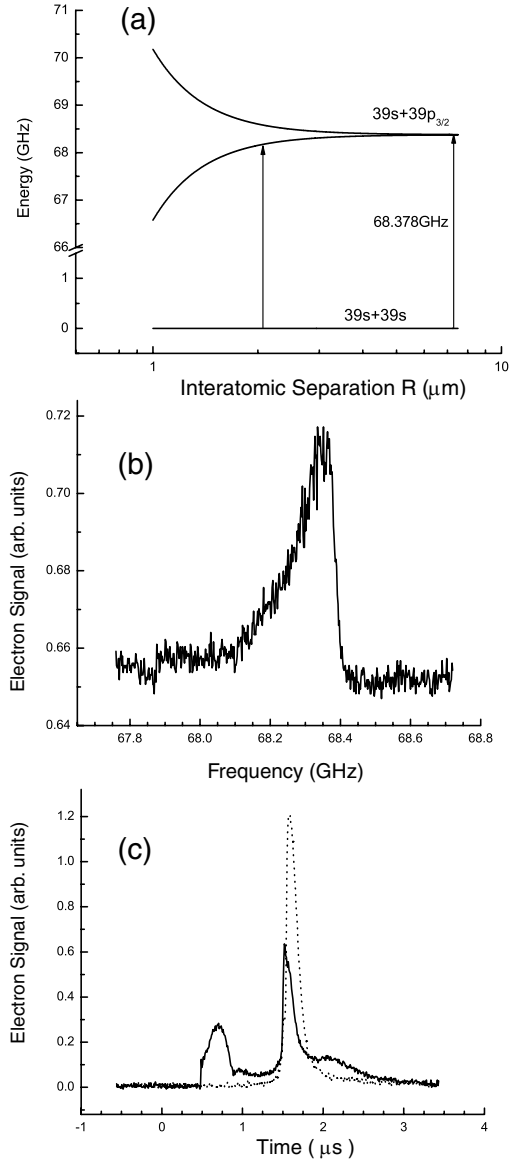

FIG. 4. (a) Energy levels for the $39s39s$-$39s39p$ transition vs interatomic spacing R. (b) Free ion signal vs microwave frequency. A signal is observed only on the low frequency side of the atomic frequency, 68.378 GHz; i.e., only transitions to the attractive curve of (a) are observed. (c) Time resolved electron signals after a 3.5 μs delay subsequent to exciting the $39s$ state with (solid line) and without (dotted line) the microwave pulse. Without the microwaves, only the $39s$ field ionization signal is observed. With the microwave, a plasma signal at 0.5 μs relative to the start of the field ionization pulse and the redistribution of the remaining Rydberg population are evident.

ing decreases as n^{-3}, ensures that the resonant $\mu\mu/R^3$ dipole-dipole interaction is dominant out to very large interatomic spacings. The measurements reported here indicate that ionization resulting from this resonant interaction is the source of the initial ionization leading to the Rydberg-plasma evolution in purely cold atom samples. We suggest that recently reported local van der Waals excitation blockades may be due in large part to the resonant dipole-dipole effect described here [20,21]. More generally, the dipole interactions between Rydberg atoms cause them to move, and this motion cannot be neglected in any proposed applications involving cold Rydberg atoms, although it may be minimized by using a regular lattice of atoms.

It is a pleasure to acknowledge useful discussions with L. A. Bloomfield, P. Pillet, L. D. Noordam, and J. D. D. Martin. This work has been supported by the Air Force Office of Scientific Research.

[1] W. R. Anderson, J. R. Veale, and T. F. Gallagher, Phys. Rev. Lett. **80**, 249 (1998).
[2] I. Mourachko, D. Comparat, F. de Tomasi, A. Fioretti, P. Nosbaum, V. M. Akulin, and P. Pillet, Phys. Rev. Lett. **80**, 253 (1998).
[3] J. S. Frasier, V. Celli, and T. Blum, Phys. Rev. A **59**, 4358 (1999).
[4] I. Mourachko, W. Li, and T. F. Gallagher, Phys. Rev. A **70**, 031401 (2004).
[5] T. J. Carroll, K. Claringbould, A. Goodsell, M. J. Lim, and M. W. Noel, Phys. Rev. Lett. **93**, 153001 (2004).
[6] K. Afrousheh, P. Bohlouli-Zanjani, D. Vagale, A. Mugford, M. Fedorov, and J. D. D. Martin, Phys. Rev. Lett. **93**, 233001 (2004).
[7] D. Jaksch, J. I. Cirac, P. Zoller, S. L. Rolston, R. Côté, and M. D. Lukin, Phys. Rev. Lett. **85**, 2208 (2000).
[8] M. D. Lukin, M. Fleischhauer, R. Côté, L. M. Duan, D. Jaksch, J. I. Cirac, and P. Zoller, Phys. Rev. Lett. **87**, 037901 (2001).
[9] M. P. Robinson, B. Laburthe Tolra, M. W. Noel, T. F. Gallagher, and P. Pillet, Phys. Rev. Lett. **85**, 4466 (2000).
[10] S. K. Dutta, D. Feldbaum, A. Walz-Flannigan, J. R. Guest, and G. Raithel, Phys. Rev. Lett. **86**, 3993 (2001).
[11] E. E. Eyler and P. L. Gould (private communication).
[12] T. C. Killian, M. J. Lim, S. Kulin, R. Dumke, S. D. Bergeson, and S. L. Rolston, Phys. Rev. Lett. **86**, 3759 (2001).
[13] W. Li, M. W. Noel, M. P. Robinson, P. J. Tanner, T. F. Gallagher, D. Comparat, B. Laburthe-Tolra, N. Vanhaecke, T. Vogt, N. Zahzam, P. Pillet, and D. A. Tate, Phys. Rev. A **70**, 042713 (2004).
[14] J. O. Hirschfelder, C. F. Curtiss, and R. B. Bird, *Molecular Theory of Gases and Liquids* (John Wiley & Sons, New York, 1954), pp. 955–964.
[15] A. Gallagher and D. E. Pritchard, Phys. Rev. Lett. **63**, 957 (1989).
[16] W. Li, I. Mourachko, M. W. Noel, and T. F. Gallagher, Phys. Rev. A **67**, 052502 (2003).
[17] M. L. Zimmerman, M. G. Littman, M. M. Kash, and D. Kleppner, Phys. Rev. A **20**, 2251 (1979).
[18] C. Monroe, W. Swann, H. Robinson, and C. Wieman, Phys. Rev. Lett. **65**, 1571 (1990).
[19] T. F. Gallagher, *Rydberg Atoms* (Cambridge University Press, Cambridge, England, 1994).
[20] D. Tong, S. M. Farooqi, J. Stanojevic, S. Krishnan, Y. P. Zhang, R. Côté, E. E. Eyler, and P. L. Gould, Phys. Rev. Lett. **93**, 063001 (2004).
[21] K. Singer, M. Reetz-Lamour, T. Amthor, L. G. Marcassa, and M. Weidemüller, Phys. Rev. Lett. **93**, 163001 (2004).